Supporting Information: Large negative linear compressibility of a porous molecular co-crystal

Szymon Sobczak,[a] Aleksandra Półrolniczak,[a] Paulina Ratajczyk, [a] Weizhao Cai,†[a] Andrzej Gładysiak,‡[a] Varvara I. Nikolayenko,[b] Dominic C. Castell,[b] Leonard J. Barbour,[b]* Andrzej Katrusiak [a]*

[a] Department of Materials Chemistry, Faculty of Chemistry, Adam Mickiewicz University, Umultowska 89b, 61-614 Poznań, Poland. E-mail: katran@amu.edu.pl

[b] Department of Chemistry and Polymer Science, University of Stellenbosch, 7600, Matieland, South Africa. E-mail: ljb@sun.ac.za

† Present address: Department of Physics and Astronomy, University of Utah, Salt Lake City, Utah 84112, United States

‡ Present address: Laboratory of Molecular Simulation (LSMO), Institut des sciences et ingénierie chimiques (ISIC), École polytechnique fédérale de Lausanne (EPFL) Valais, Rue de l'Industrie 17, 1951 Sion, Switzerland.

Experimental

Quantum mechanical optimization

For the optimization of BTCP molecular geometry in gaseous state, the density functional theory methodB3LYP was used in the Gaussian 03 program[1] with b3lyp/6-311g(d,p) basis set have been used.[2]

High-pressure Crystallography

Single-crystal X-ray diffraction data were collected at room temperature on a 4-circle Oxford-Diffraction Xcalibur Eos diffractometer with graphite monochromated MoKα radiation (λ = 0.71073 Å). Single-crystal data for co-crystal BTCP·dItFB·Ac were measured at room temperature on a SuperNova CCD Atlas diffractometer with monochromated CuKα

radiation (λ = 1.54168 Å). For all crystals the unit-cell dimensions were obtained by the program CrysAlisPro. The structures were solved with the ShelXS structure solution program using direct methods and refined by the least-squares method using ShelXL[3,4] within the Olex2 interface.[5] The quality and the completeness of the high-pressure XRD datasets were sufficient for determining the partial contents of pores and positions of solvent molecules. The two sites of the acetone molecule have approximately equal occupancies of ½.

High-pressure experiments were performed in a Merrill-Bassett diamond-anvil cell (DAC), modified by mounting the diamond anvils directly on the steel support with conical windows.[6] The gasket was made of steel foil, 0.3 mm thick, with a spark-eroded 0.4 mm hole pre-indented.[7] Glycerin was used as the pressure-transmitting medium. The pressure in the DAC was calibrated using the R_1 ruby-line shift, measured by a Photon Control Spectrometer of enhanced resolution, affording an accuracy of 0.02 Gpa.[8,9] The DAC was centered by the gasket-shadow method.[10] Experiments were performed on a four-circle Oxford-Diffraction Xcalibur Eos X-ray diffractometer equipped with an EOS-CCD detector. The high pressure structures were refined using the ambient-pressure structure of the co-crystal as a starting model. Due to strongly disordered solvent molecules in all high-pressure measurements the Platon algorithm SQUEEZE was applied.[11]

The crystallographic data and experimental details are summarized in Tables 1 and S1. CCDC 1886608-1886615.

Table S1. Molecular crystals of high negative linear compressibility (NLC) and its magnitudes

Compound	NLC value (TPa^{-1})	Reference
BTCP·dItFB·Ac	-30	This work
$[Fe(dpp)_2(NCS)_2]\cdot py$	−10.3	[12]
$[(C_6F_5Au)_2(\mu\text{-}1,4\text{-diisocyanobenzene})]$	−12.57	[13]
Methyl Benzoate	–16.5(3)	[14]
$(NH_4)_2C_2O_4\cdot H_2O$	–2.3(7)	[15]
ROY	–5.5(8)	[16]
Methanol monohydrate	–3.8(5)	[17]
3-Methyl 4-nitropyridine 1-oxide	-33(2)	[18]
$Cd(COOH)_2$	-0.26	[19]
$Ca(COOH)_2$	-0.21	[19]
m-Dihydroxybenzene	-0.18	[19]
$C_6H_4COOHCOOCs$	-0.1	[19]
$(CH_3NHCH_2COOH)_3CaCl_2$	-0.07	[19]
$C_6H_{14}N_2O_6$	-0.1	[19]
3-methyl-4-nitropyridine N-oxide	-0.44	[19]
2-MeBzIm	-15(6)	[20]

Table S2. Conformational changes of the BTCP molecule as a response to hydrostatic pressure.

p (GPa)	py–py distance (Å)	py–cp–py angle (°)
Calculated molecule	12.459	11.85
0.0001	12.517	117.12
0.4	12.567	118.12
0.7	12.724	120.02
1.09	12.799	121.09
1.59	12.899	120.59
1.95	12.819	120.50

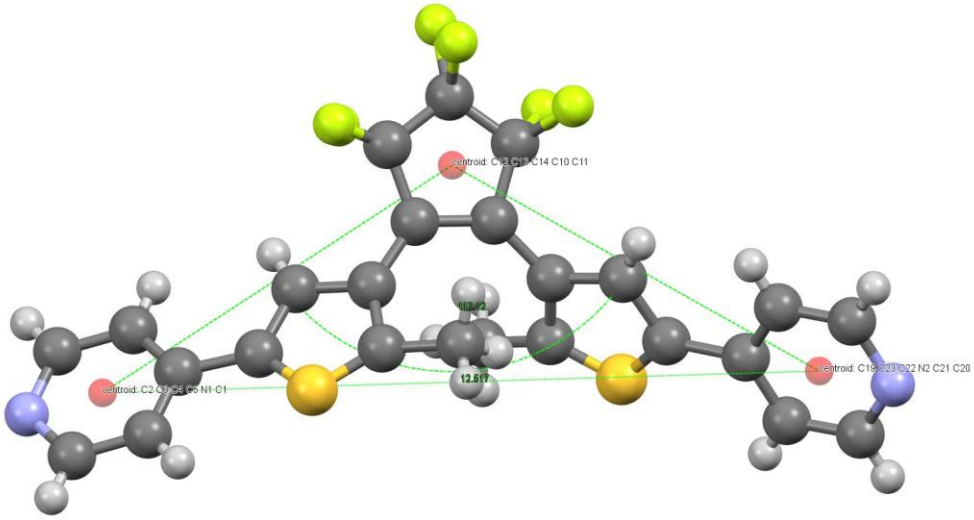

Figure S1. Measurement of the py–py distance and the py–cp–py angle in the BTCP molecule at 0.0001 GPa.

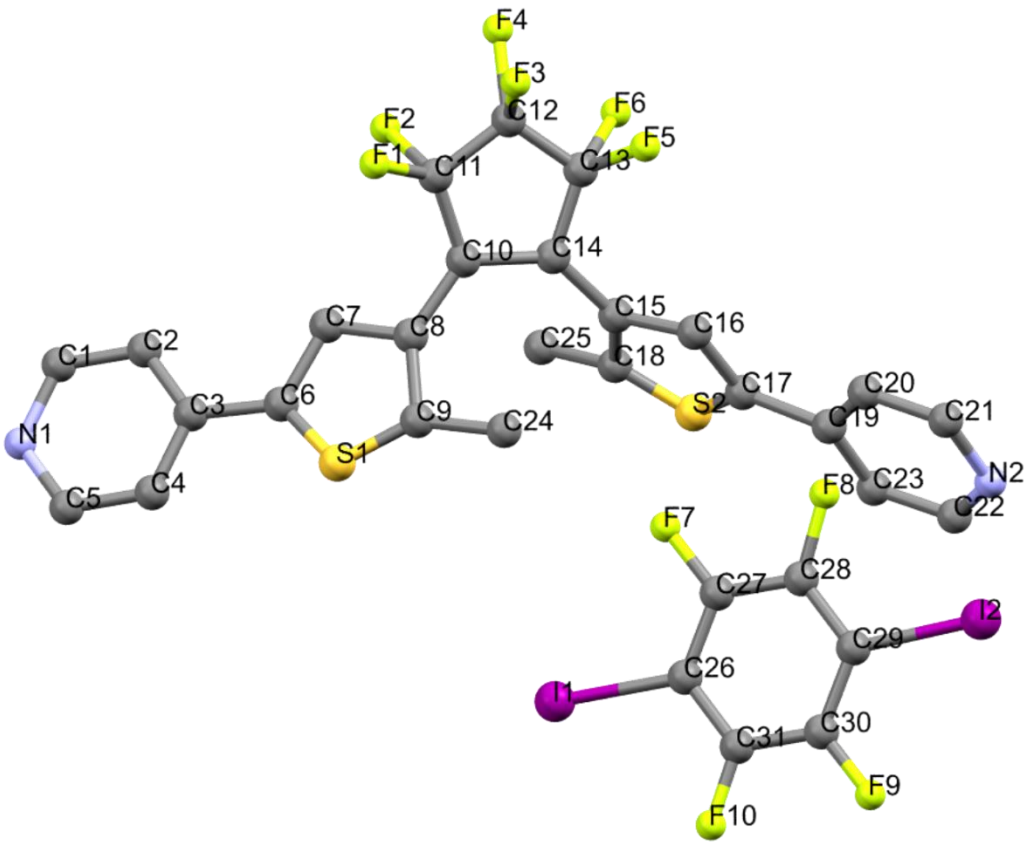

Figure S2. The asymmetric unit of BTCP·dItFb with the acetone molecule omitted for clarity.

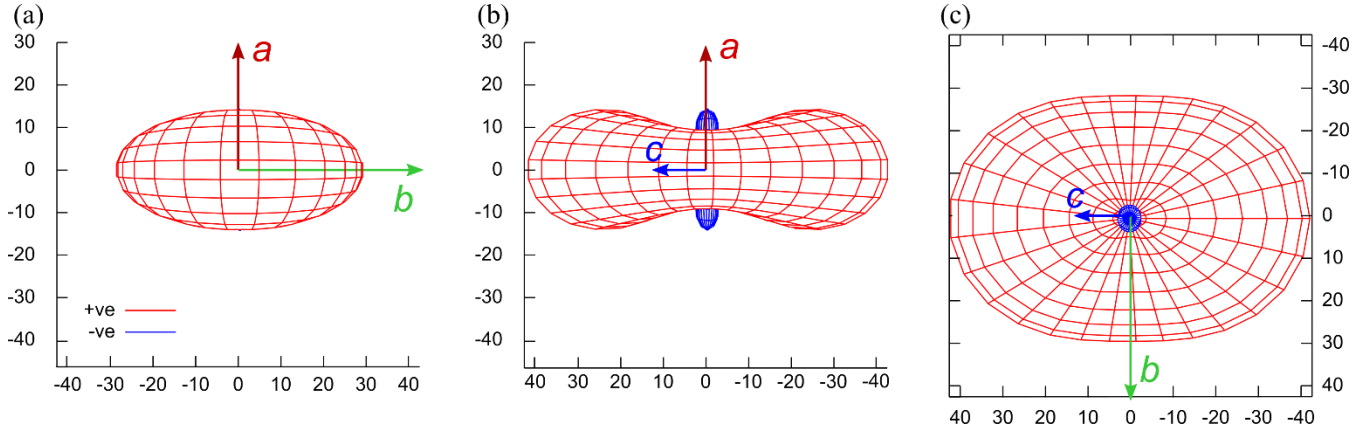

Figure S3. Calculated compressibility (in TPa^{-1}) indicatrices of co BTCP·dItFB·Ac in pressure between 0.1 MPa and 0.4 GPa viewed along the (a) [100] (b) [010] and (c) [010] directions .

Table S3. Compressibility related to crystallographic axes calculated for BTCP·dItFB·Ac in a pressure range between 0.1 MPa and 0.7 GPa.

			Direction			Empirical parameters			
Axes	***K*(TPa^{-1})**	**σ*K*(TPa^{-1})**	***a***	***b***	***c***	ε_0	λ	P_c	***v***
X_1	X_1	89.2728	0.0000	0.0000	0.0000	1.0000	0.0000e+00	0.0000e+00	0.0000
X_2	X_2	60.6307	0.0000	0.0000	1.0000	-0.0000	0.0000e+00	0.0000e+00	0.0000
X_3	X_3	-29.2754	0.0000	1.0000	0.0000	-0.0000	0.0000e+00	0.0000e+00	0.0000
V	**V**	117.8123	0.0000						

Birch-Murnaghan Coefficients

	B_0 (GPa)	σB_0 (GPa)	V_0 (Å^3)	σV_0 (Å^3)	B'	$\sigma B'$	P_c (GPa)
2nd	7.5234	inf	3726.4671	inf	4	n/a	0

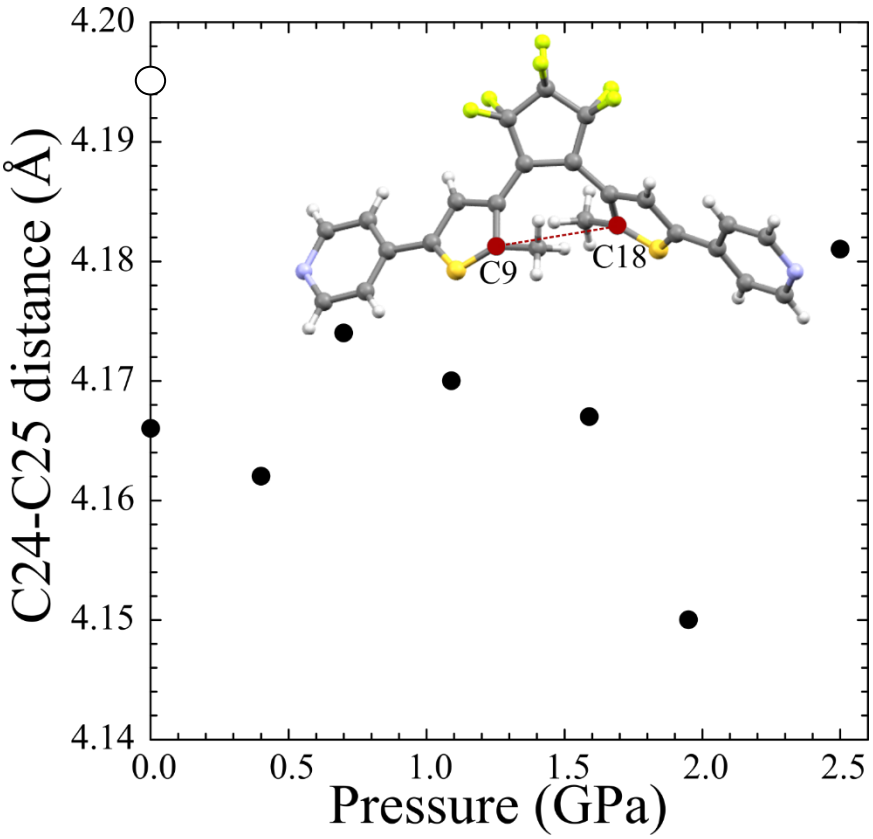

Figure S4. Changes in the distance between C9 and C18 in BTCP presented in the function of pressure. ESDs are smaller than the plotted symbols. Open symbol marks the measurement after immersion in water.

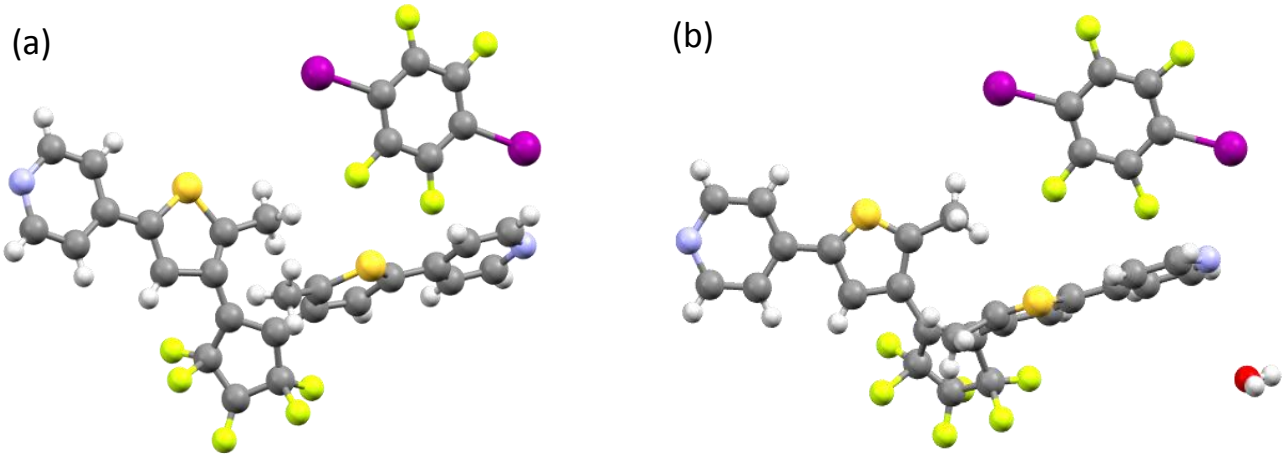

Figure S5. Conformation of **BTCPs** molecule a) in co-crystal BTCP·dItFB·Ac at ambient pressure b) in co-crystal BTCP·dItFB·Ac at 2.5 GPa.

References

1 M. J. Frisch, G. W. Trucks, H. B. Schlegel, G. E. Scuseria, M. A. Robb, J. R. Cheeseman, J. A. Montgomery Jr., T. Vreven, K. N. Kudin, J. C. Burant, J. M. Millam, S. S. Iyengar, J. Tomasi, V. Barone, B. Mennucci, M. Cossi, G. Scalmani, N. Rega, G. A. Petersson, H. Nakatsuji, M. Hada, M. Ehara, K. Toyota, R. Fukuda, J. Hasegawa, M. Ishida, T. Nakajima, Y. Honda, O. Kitao, H. Nakai, M. Klene, X. Li, J. E. Knox, H. P. Hratchian, J. B. Cross, V. Bakken, C. Adamo, J. Jaramillo, R. Gomperts, R. E. Stratmann, O. Yazyev, A. J. Austin, R. Cammi, C. Pomelli, J. W. Ochterski, P. Y. Ayala, K. Morokuma, G. A. Voth, P. Salvador, J. J. Dannenberg, V. G. Zakrzewski, S. Dapprich, A. D. Daniels, M. C. Strain, O. Farkas, D. K. Malick, A. D. Rabuck, K. Raghavachari, J. B. Foresman, J. V Ortiz, Q. Cui, A. G. Baboul, S. Clifford, J. Cioslowski, B. B. Stefanov, G. Liu, A. Liashenko, P. Piskorz, I. Komaromi, R. L. Martin, D. J. Fox, T. Keith, M. A. Al-Laham, C. Y. Peng, A. Nanayakkara, M. Challacombe, P. M. W. Gill, B. Johnson, W. Chen, M. W. Wong, C. Gonzalez and J. A. Pople, 2004.

2 K. B. Wiberg, *J. Comput. Chem.*, 2004, **25**, 1342–1346.

3 G. M. Sheldrick, *Acta Crystallogr. Sect. C Struct. Chem.*, 2015, **71**, 3–8.

4 G. M. Sheldrick, *Acta Crystallogr. Sect. A Found. Crystallogr.*, 2008, **64**, 112–122.

5 O. V. Dolomanov, L. J. Bourhis, R. J. Gildea, J. A. K. Howard and H. Puschmann, *J. Appl. Crystallogr.*, 1999, **32**, 1021–1023.

6 L. Merrill and W. A. Bassett, *Rev. Sci. Instrum.*, 1974, **45**, 290–294.

7 A. Katrusiak, *J. Appl. Crystallogr.*, 1999, **32**, 1021–1023.

8 G. J. Piermarini, S. Block, J. D. Barnett and R. A. Forman, *J. Appl. Phys.*, 1975, **46**, 2774–2780.

9 H. K. Mao, J. Xu and P. M. Bell, *J. Geophys. Res.*, 2008, **91**, 4673.

10 F. Chemistry, *High Press. Crystallogr.*, 2004, **140**, 101–112.

11 A. L. Spek, *Acta Crystallogr. Sect. C Struct. Chem.*, 2015, **71**, 9–18.

12 H. J. Shepherd, T. Palamarciuc, P. Rosa, P. Guionneau and G. Molnár, *Angew. Chem.*, 2012, **51**, 3910-3914.

13 C. H. Woodall, C. M. Beavers, J. Christensen, L. E. Hatcher, M. Intissar, A. Parlett, S. J. Teat, C. Reber and P. R. Raithby, *Angew. Chemie - Int. Ed.*, 2013, **52**, 9691–9694.

14 W. Cai and A. Katrusiak, *J. Phys. Chem. C*, 2013, **117**, 21460–21465.

15 Y. Qiao, K. Wang, H. Yuan, K. Yang and B. Zou, *J. Phys. Chem. Lett.*, 2015, **6**, 2755–2760.

16 E. L. Harty, A. R. Ha, M. R. Warren, A. L. Thompson, D. R. . Allan, A. L. Goodwin and N. P. Funnell, *Chem. Commun.*, 2015, **51**, 10608–10611.

17 A. D. Fortes, E. Suard and K. S. Knight, *Science (80-.).*, 2011, **331**, 742–746.

18 W. Cai, J. He, W. Li and A. Katrusiak, *J. Mater. Chem. C*, 2014, **2**, 6471–6476.

19 R. H. Baughman, S. Stafstro, C. Cui and S. O. Dantas, *Science*, 1998, **279**, 1522–1524.

20 W. Zieliński and A. Katrusiak, *Cryst. Growth Des.*, 2014, **14**, 4247–4253.

Table S4. Detailed crystallographic information for BTCPs·dItFB co-crystal compressed in glycerol

Pressure		0.1 MPa	0.1 MPa H_2O	0.4 GPa	0.7 GPa	1.09 GPa	1.59 GPa	1.95 GPa	2.5 GPa
CCDC numbers		1886608	1886609	1886610	1886611	1886614	1886612	1886613	1886615
Formula weight		982.45	998.7	924.38	924.38	924.38	924.38	942.39	942.39
Chemical formula		$C_{34}H_{22}F_{10}I_2N_2OS_2$	$C_{33.85}H_{24}F_{10}I_2N_2O_2S_2$	$C_{31}H_{16}F_{10}I_2N_2S_2$	$C_{31}H_{16}F_{10}I_2N_2S_2$	$C_{31}H_{16}F_{10}I_2N_2S_2$	$C_{31}H_{16}F_{10}I_2N_2S_2$	$C_{31}H_{18}F_{10}I_2N_2OS_2$	$C_{31}H_{18}F_{10}I_2N_2OS_2$
Wavelength (Å)		0.71073	0.71073	0.71073	0.71073	0.71073	0.71073	0.71073	0.71073
Crystal system		orthorhombic	orthorhombic	orthorhombic	orthorhombic	orthorhombic	orthorhombic	orthorhombic	orthorhombic
Space group		P*na2(1)*	P*na2(1)*	P*na2(1)*	P*na2(1)*	P*na2(1)*	P*na2(1)*	P*na2(1)*	P*na2(1)*
Unit cell dimensions	a (Å)	17.2715(8)	17.2451(6)	17.556(4)	17.449(4)	17.559(5)	17.723(8)	17.564(10)	17.606(3)
	b (Å)	27.171(3)	27.2415(16)	26.464(17)	26.511(15)	26.315(16)	26.15(6)	25.64(4)	25.580(17)
	c (Å)	7.9406(7)	7.9554(3)	7.633(2)	7.536(11)	7.259(8)	7.00(3)	7.07(3)	6.944(9)
Volume ($Å^3$)		3726.4(6)	3737.3(3)	3546(3)	3486(5)	3354(4)	3242(18)	3185(15)	3127(5)
Z/Z'		4/1	4/1	4/1	4/1	4/1	4/1	4/1	4/1
Molecular volume (V/Z)		931.6	934.32	886.5	871.5	838.5	810.5	796.25	781.75
Calculated density (g/cm^3)		1.751	1.775	1.731	1.761	1.831	1.894	1.966	2.002
Absorption (mm^{-1})		1.880	1.878	1.968	2.002	2.080	2.152	2.195	2.236
F(000)		1904.0	1940.0	1776.0	1776.0	1776.0	1776.0	1816.0	1816.0
Crystal size (mm)		0.325 × 0.102 × 0.046	0.327 × 0.103 × 0.046	0.325 × 0.103 × 0.046	0.324 × 0.104 × 0.046	0.324 × 0.104 × 0.046	0.323 × 0.105 × 0.046	0.322 × 0.105 × 0.046	0.322 × 0.106 × 0.046
2θ-range for data collection (°)		5.842 to 52.732	5.834 to 52.738	7.614 to 49.42	8.39 to 52.706	8.372 to 49.426	8.334 to 50.052	8.44 to 31.704	8.432 to 29.396
Min/max indices: h, k, l		-21/21, -33/33, -9/9	-21/21, -34/34, -9/9	-20/20, -23/22, -8/8	-21/21, -29/29, -5/5	-20/20, -28/28, -6/5	-21/21, -27/27, -5/5	-13/13, -18/19, -4 /4	-12/12, -17/16, -3/3
Reflect. Collected/unique		57440/7588	44072/7610	18081/3900	15662/3251	15625 /3321	14627/2530	6062/992	5210/786
Rint		0.1674	0.0942	0.2456	0.2550	0.2726	0.3185	0.2608	0.2913
Refinement method		Full-matrix least-squares on F2							
Completeness (%)		100	100	64	50	57	44	66	67
Data/restrains/parameters		7588/885/421	7610/588/452	3900/700/363	3251/895/363	3321/694/351	2530/848/363	992/777/370	786/916/393
Goodness-of-fit on F2		1.108	1.078	1.096	1.011	1.070	1.055	1.772	1.724
Final R1/wR2 (I>2σ1)		0.1685/0.3775	0.1190/0.2469	0.2025/0.4301	0.1399/ 0.3503	0.1781/0.3875	0.1738/0.3915	0.1726/0.4108	0.1421/0.3450
R1/wR2 (all data)		0.2522/0.4266	0.1592/0.2726	0.4824/0.5737	0.3835/0.4872	0.4167/0.5136	0.4345/0.5193	0.2562/0.4820	0.2098/0.4147
Largest diff. peak/hole (e.Å-3)		2.03/-2.15	1.38/-1.22	1.04/-0.88	0.80/-0.56	0.75/-0.64	0.97/-0.58	0.73/-0.68	0.76/-0.56

$w=1/(\sigma^2 F_o^2+w_1^2*P^2+w_2*P)$, where $P=(\mathrm{Max}(F_o^2,0)+2*F_c^2)$